Stability of zinc stearate under alpha irradiation in the manufacturing process of SFR nuclear fuels

J Gracia, J Vermeulen, D Baux, T Sauvage, L Venault, F. Audubert, X Colin

Stability of zinc stearate under alpha irradiation in the manufacturing process of SFR nuclear fuels

J. Gracia[a,b], J. Vermeulen[b], D. Baux[c], T. Sauvage[c], L. Venault[b,*], F. Audubert[a], X. Colin[d]

[a] CEA, DEN, DEC, Centre de Cadarache, F-13115 Saint Paul lez Durance, France
[b] CEA, DEN, DMRC, Centre de Marcoule, F-30207 Bagnols-sur-Cèze Cedex, France
[c] CEMHTI, CNRS UPR3079, Université d'Orléans, F-45071 Orléans Cédex 2, France
[d] Ecole Nationale Supérieure des Arts et Métiers ParisTech, PIMM, 151 Boulevard de l'Hopital, F-75013 Paris, France

ARTICLE INFO

Keywords:
MOX fuels
Zinc stearate
Plutonium dioxide
Alpha radiolysis
Gas formation yield
LET effect

ABSTRACT

The manufacture of new fuels for sodium-cooled fast reactors (SFRs) will involve powders derived from recycling existing fuels in order to keep on producing electricity while saving natural resources and reducing the amount of waste produced by spent MOX fuels. Using recycled plutonium in this way will significantly increase the amount of ^{238}Pu, a high energy alpha emitter, in the powders. The process of shaping powders by pressing requires the use of a solid lubricant, zinc stearate, to produce pellets with no defects compliant with the standards. The purpose of this study is to determine the impact of alpha radiolysis on this additive and its lubrication properties. Experiments were conducted on samples in contact with PuO_2, as well as under external helium ion beam irradiation, in order to define the kinetics of radiolytic gas generation. The yield results relating to the formation of these gases (G_0) show that the alpha radiation of plutonium can be simulated using external helium ion beam irradiation. The isotopic composition of plutonium has little impact on the yield. However, an increased yield was globally observed with increasing the mean linear energy transfer (LET). A radiolytic degradation process is proposed.

1. Introduction

The manufacturing process for nuclear fuels is based on a powder metallurgy process which usually involves the use of organic additives for the mixing, pressing and/or sintering stages.

The powder or granule compression stage introduces various phenomena such as particle rearrangement, compaction, restructuring and potential plastic deformation (Pizette et al., 2010). A full description of the compacting process must take account of the effects of friction not only between the powder and the matrix but also between the particles. The use of an additive as a lubricant helps reduce these friction forces during pressing and results in more homogeneous, better quality compacted powders. Friction is essentially responsible for creating stress gradients in the product, which form a heterogeneous density distribution that may be preserved in the end pellet after sintering. Pressing also requires a smooth powder flow and homogeneous filling of the matrix or mould to ensure uniform, reproducible densities.

Mean deformation plays a part in the demoulding process along the axial plane given that the compacted powder is contained in the matrix. This elastic expansion occurs during demoulding. If it exceeds a critical value, the sample may develop cracks in the laminations when it is ejected from the matrix.

The manufacture of future SFR fuels, and more specifically ASTRID fuels, is based on a direct co-milling of UO_2 and PuO_2 powders using a zinc stearate additive in the pressing stage.

Compared with pressurised water reactor (PWR) fuels, these new fuels will have a much higher plutonium content (target content ≈ 30% Pu *vs* Pu content < 12% in PWR MOX fuels) with a far higher concentration of highly radioactive isotopes (^{238}Pu, ^{241}Pu) due to the greater number of fuel irradiation cycles associated with a change in the isotopic vector of plutonium. Consequently, the dose deposited, mainly due to the α radiation of ^{238}Pu and ^{241}Am, will increase.

The lubricating properties of zinc stearate may be degraded by the radiolysis reaction in the presence of alpha radiation. Radiolysis is characterised by the cleavage of one or more chemical bonds caused by ionising radiation (Spinks, 1990, Balanzat et al., 1995). For an organic material (or polymer), the energy deposited in the material causes excitation and ionisation, which in turn leads to the formation of radicals (Spinks, 1990, Ferry et al., 2016). These radicals then react by recombining to form stable defects in the material. Radical reactions can be unimolecular or bimolecular. Eventually, the cleavage of the chemical bonds in solid matter can lead to the formation of gaseous

* Corresponding author.
E-mail address: laurent.venault@cea.fr (L. Venault).

Table 1
Molar isotopic compositions, total dose rate and alpha dose rates emitted by the different batches of plutonium used in this work.

Pu batch	^{238}Pu	^{239}Pu	^{240}Pu	^{241}Pu	^{242}Pu	Total dose rate emitted by PuO_2 (J kg^{-1} s^{-1})	α dose rate emitted by PuO_2 (J kg^{-1} s^{-1})	Config.
1	0.04	95.77	3.70	0.14	0.35	2.05	2.02	Plane-plane
2	1.18	0.65	14.38	0.99	82.80	6.93	6.75	Plane-plane
3	0.05	87.86	11.61	0.21	0.27	2.45	2.40	Plane-plane
4	0.78	13.98	12.95	0.50	71.79	5.01	4.88	Mixture
5	2.89	68.75	22.14	2.33	3.89	17.3	17.0	Plane-plane Mixture

compounds. If these gases remain trapped within the material, radiolysis will cause the sample to swell, which could be detrimental to the fuel shaping and sintering processes.

Zinc stearate is widely used in the nuclear industry, yet there have been very few studies into its resistance to radiation. Initial studies were conducted recently under gamma irradiation on magnesium stearate (Lebeau et al., 2015) and zinc stearate (Lebeau et al., 2017). To date, no similar studies have been conducted on the radiolysis of zinc stearate under alpha irradiation. As for many carbonyl organic compounds, the major gaseous degradation products of zinc stearate will probably be dihydrogen H_2 and carbon oxides CO_2 and CO (Spinks, 1990). Due to its structure the mechanism of the radiatolytical degradation of zinc stearate can be approached through the knowledge of radiation chemistry of polyethylene for H_2 generation from the aliphatic chain (Chang and Laverne, 2000) and of carboxylic acids for carbon oxides formation (Nawar, 1978). Alpha radiolysis of zinc stearate should lead to higher yields of the gas products in comparison to the ones obtained in gamma radiolysis (Spinks, 1990).

The purpose of this study is to investigate the behaviour of zinc stearate during radiolysis under two different types of alpha radiation: one emitted by a plutonium dioxide powder (PuO_2) and the other generated by a particle accelerator.

Studying the radiolysis of zinc stearate in contact with PuO_2 specifically will help to determine the degradation caused to lubricants in fuel manufacture, since plutonium is the main contributor to the alpha particles emission in the ASTRID fuel. Monitoring the radiolytic gases released by internal or external alpha irradiation will provide an initial analysis of the radiolytic stability of zinc stearate.

2. Experimental section

2.1. Irradiation devices

The zinc stearate was irradiated in two different ways: in contact with PuO_2 and by external helium ion beam irradiation. The internal irradiations were conducted using PuO_2 either in pellet form, by stacking alternate layers of zinc stearate and plutonium dioxide pellets (in a plane-plane configuration), or in powder form, by mixing a low mass (1–2%) of zinc stearate powder with the plutonium dioxide powder (mixture configuration). The external helium ion beam irradiations were conducted on stearate pellets at the CEMHTI research facility[1] of CNRS (French National Centre for Scientific Research) in Orléans.

2.2. Materials

The zinc stearate $(C_{18}H_{35}O_2)_2Zn$ was supplied by Alfa Aesar. For the radiolysis tests in contact with PuO_2, 150 mg of stearate powder was pressed under a pressure of 55 MPa to produce pellets 13 mm in diameter and 1 mm thick. For the external radiolysis tests conducted in the CEMHTI cyclotron, pellets 20 mm in diameter and 5 mm thick were produced by pressing 1.5 g of powder at 20 MPa. The pressing was proceeded only once for each pellet.

The plutonium oxide used for the tests in plane-plane configuration was shaped in the form of a disc, 13 mm in diameter and 200 μm thick (using ~ 350 mg of powder). Several plutonium isotopic composition were used in this study (Table 1) in order to characterise the effect of a variation in plutonium alpha activity on the radiolytic degradation of zinc stearate.

The mean dose rate delivered by a gram of plutonium, expressed in J kg^{-1} s^{-1}, is calculated using the following equation (Eq. (1)) (Vladimirova and Kulikov, 2012):

$$\dot{D}_{Pu} = \sum_i f_{i,\alpha} E_{i,\alpha} A_{i,\alpha} + \sum_i f_{i,\beta} E_{i,\beta} A_{i,\beta} \quad (1)$$

Where $f_{i,\alpha}$: Mass fraction of the isotope i for the α irradiations

$f_{i,\beta}$: Mass fraction of the isotope i for the β irradiations
$E_{i,\alpha}$: Energy of the α particle emitted by the isotope i (J)
$E_{i,\beta}$: Energy of the β particle emitted by the isotope i (J)
$A_{i,\alpha}$: Specific α activity of the isotope i (Bq kg^{-1})
$A_{i,\beta}$: Specific β activity of the isotope i (Bq kg^{-1})

Values of specific activity and energy of α and β particles are given in Table 2 for each isotope of plutonium.

Alpha decay is the main contributor in plutonium radioactivity. Only 2–4% of the total dose rate emitted comes from the beta particles produced by the radioactive disintegration of ^{241}Pu.

The mean dose rate emitted per gram of PuO_2 (J kg^{-1} s^{-1}) is obtained by multiplying the mean dose rate emitted per gram of Pu by the molar mass ratio M_{Pu}/M_{PuO2} (Eq. (2)).

$$\dot{D}_{PuO_2} = M_{Pu}/M_{PuO_2} \text{ x } \dot{D}_{Pu} \quad (2)$$

Batches 1, 2, 3 and a part of batch 5 are used in plane-plane configuration, and batch 4 and the rest of batch 5 is used in mixture configuration.

2.3. Radiolysis experiments and gas analysis

Radiolysis of the zinc stearate in contact with PuO_2 powders was carried out in gas-tight cells equipped with a system of gas sampling valves. This allows samples for analysis to be kept in a controlled atmosphere and to contain the gases produced during radiolysis. The atmosphere in the cells is Ar/1% Ne, where neon is used as standard for gas-chromatography analysis. The cell was made of borosilicate glass and the seals and valve fittings were made of PTFE (polytetrafluoroethylene).

Table 2
LNHB data for energies and specific activities of plutonium isotopes.

Isotope	^{238}Pu	^{239}Pu	^{240}Pu	^{241}Pu	^{242}Pu
A_α (10^{12} Bq kg^{-1})	633.44	2.30	8.40	–	0.15
E_α (10^{-13} J)	8.961	8.403	8.421	–	7.986
A_β (10^{12} Bq kg^{-1})	–	–	–	3830.11	–
E_β (10^{-13} J)	–	–	–	0.003	–

[1] *Research facility for studying materials in extreme conditions: high temperature and irradiation.*

Table 3
Characteristics of the stacks used for the plane-plane radiolysis experiments.

PuO_2	Organic compound	Mass of PuO_2 powder (g)	Number of PuO_2 discs	Number of interfaces	Energy rate $\dot{E}_\alpha$ (10^{-6} J s^{-1})	Absorbed dose rate (J kg^{-1} s^{-1})
Batch 1	Zinc stearate	1.666	5	10	86.2	1.74
Batch 2	Zinc stearate	1.827	5	10	315.6	6.36
Batch 3	Zinc stearate	1.396	4	8	86.5	2.17
Batch 5	Zinc stearate	0.646	2	4	282.0	14.20

For external irradiations, the powders were irradiated by helium ion particle beam in a vessel capable of containing the target material and the radiolytic gases produced, whilst allowing the particle beam to pass through horizontally. The pellet was held in a vertical position perpendicular to the beam axis. The radiolysis cell and support were made from PEEK (polyetheretherketone). A borosilicate glass disc (20 mm in diameter) was used as a window for the particle beam to pass through. The glass disc was 145 ± 15 µm thick (38.7 mg cm^{-2}). The cell was gas-tight and equipped with a device for removing an aliquot of the gaseous atmosphere for analysis. The radiolysis cells were conditioned in an inert atmosphere (Ar/1% Ne) at the initial pressure of 1.2 × 10^5 Pa.

The composition of the gaseous atmosphere in the cells was determined by removing an aliquot at given times for micro gas-chromatography analysis using a 3000 Micro-GC connected to an Agilent 5975C mass spectrometer supplied by SRA instruments. The detector for the micro-GC was a micro-katharometer (Thermal Conductivity Detector - TCD) also supplied by SRA Instruments. During the analyses, the chromatography columns were maintained at 45 °C. Four columns were used: a 5 Å molecular sieves, a PoraPlot U, a PoraPlot Q and an OV-1. The columns were reconditioned at 180 °C regularly to eliminate all the impurities caused by irreversible adsorption at low temperatures. Samples were injected via a 17 µl injection loop.

2.4. Determining the energy/dose absorbed by the zinc stearate

2.4.1. Irradiations by PuO_2 in a plane-plane configuration

The alternate stacking of zinc stearate and PuO_2 pellets provides a controlled geometry and an easy way of calculating the energy absorbed by the stearate whilst maximising the irradiated surface.

The alpha energy release rate (J s^{-1}) at each PuO_2/zinc stearate interface ($\dot{E}_{\alpha_{released\ per\ interface}}$) is calculated using the following equation (Eq. (3)):

$$\dot{E}_{\alpha_{released\ per\ interface}} = \dot{D}_{PuO_2} \cdot \rho_{PuO_2} \cdot \frac{V_{pellet}}{2} \cdot (1-b) \quad (3)$$

where ρ_{PuO_2}: Density of PuO_2 (g cm^{-3})

V_{pellet}: Volume of a PuO_2 pellet (cm^3)

(1-b): Correction factor for the proportion of alpha particles transferring from the PuO_2 pellet to the zinc stearate

Irrespective of which plutonium batch is used in this study, there is very little variation in the rate of self-absorption with thickness. Particles lost from the edges of the discs (slices) are disregarded in terms of the dimensions of the PuO_2 discs. The computational code takes account of the fact that not all the particles are emitted with the same energy (originating from different thicknesses, with different paths), and compensates for this parameter in the self-absorption value used. A fixed self-absorption value b = 0.986 ± 0.002 was used for the absorbed energy calculations.

This energy rate is multiplied by the number of PuO_2/StZn interfaces present in the stack to obtain the total energy rate. The number of interfaces depends on the number of PuO_2 discs it that was possible to produce from the quantities of powder available after purification and calcination of the batches. Assuming that the path of α particles emitted by plutonium in zinc stearate is 34 µm as calculated by SRIM-2008 software, the mass of zinc stearate irradiated and then the dose rate absorbed by zinc stearate can be evaluated. The volume of zinc stearate irradiated at each interface of the pellets corresponds to a cylinder of 1.3 mm diameter and 34 µm thick. Then the mass of zinc stearate irradiated at each interface is m = 4.96 mg, assuming a volume weight ρ = 1.1 g cm^{-3} for zinc stearate. Knowing the energy rate for each sample, the mean dose rate absorbed by zinc stearate can be calculated. Table 3 summarises the characteristics of each stack studied.

2.4.2. Irradiation by PuO_2 in a mixture configuration

The zinc stearate/PuO_2 powder mixture is more representative of the use of powders in the fuel manufacturing process. It is, however, more complicated to determine the dose absorbed by the small amount of stearate present in a PuO_2 matrix. It is assumed that the stearate is distributed homogeneously after mixing.

A calculation method which takes into account the local distribution of energy released in the mixture is used to determine the dose rate absorbed by a grain of stearate in contact with a grain of PuO_2. The simulation can be adapted according to the shape (spherical or chip-shaped) and size of the oxide grains, and the size of the stearate grains (quantity present around the oxide grain). To estimate the mean dose rate deposited in the stearate grain, a calculation is performed which assumes that the stearate is in the form of a layer of $2R_{StZn}$ thick (Fig. 1). All the grains (PuO_2 and zinc stearate) are assumed to be spherical.

The software calculates the dose rate as a function of the distance r from the source (d(r)). The mean dose rate deposited by a grain of PuO_2 ($\dot{D}_{1grain}$) represents the total energy deposited in a layer with a thickness $2R_{StZn}$ divided by the mass of this layer (Eq. (4)):

$$\dot{D}_{1\,grain}(R_{StZn}, R_{grain}) = \frac{\int_0^{2R_{StZn}} d(r) \cdot \frac{4 \cdot \pi}{3} \cdot \rho_{StZn} \cdot [(r + R_{grain})^3 - R_{grain}^3] \cdot dr}{\frac{4 \cdot \pi}{3} \cdot \rho_{ZnSt} \cdot [(2R_{StZn} + R_{grain})^3 - R_{grain}^3]} \quad (4)$$

To determine the total dose rate deposited in a grain of zinc stearate,

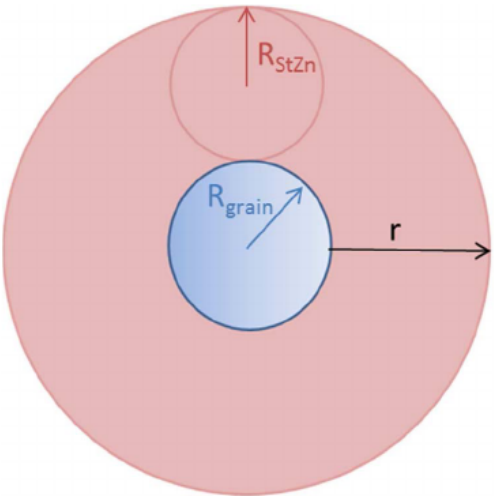

Fig. 1. "Embedded grain" configuration in the 3DiP software used to calculate the mean dose rate deposited by a grain of PuO_2 in a grain of zinc stearate with a radius R_{StZn}.

this mean dose rate must be multiplied by the number of grains of PuO_2 in contact with the stearate grain. To determine this number, one must first define the maximum possible number of PuO_2 spheres that can surround a grain of zinc stearate. The size of the stearate grains (tri-modal distribution of 3, 11 and 20 μm) and PuO_2 grains (10 μm) were determined by grain size distribution.

The number of PuO_2 grains in contact with the zinc stearate is determined using the equation below (Eq. (5)):

$$N_{grains}(R_{StZn}, R_{grain}) = \frac{\frac{4\cdot\pi}{3}\cdot[(R_{ZnSt}+2R_{grain})^3 - R_{StZn}^3]}{\frac{4\cdot\pi}{3}\cdot R_{grain}^3} \quad (5)$$

For each zinc stearate grain size, the value N_{grains} must be rounded down since the number of PuO_2 grains must be a whole number. To determine the mean number of grains ($N_{mean\ grains}$) in contact with a grain of zinc stearate, the value of N_{grains} for each zinc stearate grain size is weighted by the volume particle size distribution of each grain. This value is compared to the ratio of the number of PuO_2 grains to the number of StZn grains, which is calculated according to (Eq. (6))

$$p(R_{StZn}, R_{grain}) = \frac{N_{grains\ PuO2}}{N_{grains\ StZn}} = \frac{m_{PuO2}\rho_{PuO2}\cdot(\frac{4\cdot\pi}{3}\cdot R_{grain}^3)}{m_{StZn}\cdot\rho_{StZn}\cdot(\frac{4\cdot\pi}{3}\cdot\sum_i f_i R_i^3)} \quad (6)$$

Where m_{PuO_2}: Mass of PuO_2 used (g)

m_{StZn}: Mass of zinc stearate added to the PuO_2 (g)
ρ_{PuO_2}: Density of PuO_2 (g cm^{-3})
f_i: Volume percent of a zinc stearate grain of size i
R_i: Radius of the zinc stearate grain of size i (cm^3)

If the value of $N_{mean\ grains}$ determined is less than the ratio of the number of grains $p(R_{StZn}, R_{grain})$, the mean dose rate must be calculated for the mixture using the following equation (Eq. (7)):

$$\dot{D}_{mean\ total} = \dot{D}_{1\ grain}\cdot N_{mean\ grains} \quad (7)$$

If the value of $N_{mean\ grains}$ is greater than the ratio p, the mean dose rate is calculated as follows (Eq. (8)):

$$\dot{D}_{mean\ total} = \dot{D}_{1\ grain}\cdot p \quad (8)$$

The total mean dose rates determined by this calculation method for batches 4 and 5 are given in Table 4.

2.4.3. Helium ion beam irradiation

The $^4He^{2+}$ particles are produced with an initial energy of 28 or 45 MeV. The particles lose some of their energy as they pass through the titanium thin walls of ionisation chamber and the borosilicate glass window of the PEEK cells. The residual energy of particles arriving at the sample is calculated using SRIM-2008 software and equals 7.9 ± 2.0 and 34 ± 1.0 MeV respectively.

The total charge deposited on the sample during irradiation is measured using an ionisation chamber placed on the beam line upstream of the sample. A calibration process conducted prior to the irradiations is used to determine the proportionality constant R between the current deposited on the target and that measured at the ionisation chamber. The number of $^4He^{2+}$ particles that have interacted with the sample during irradiation is calculated as follows (Eq. (9)):

$$N_{helium\ ions} = \frac{\frac{C_{ionisation\ chamber}}{R}}{2\cdot|e|} \quad (9)$$

$C_{ionisation\ chamber}$: Charge produced in the ionisation chamber during irradiation of duration t
R: Ratio of $I_{Ionisation\ Ch.}/I_{Target}$
| e |: Elementary charge of one electron (1.602 × 10^{-19} C). Given that the sample was irradiated by helium ions (He^{2+}), the charge on the surface of the pellet is divided by twice the elementary charge to obtain the number of helium ions impacting the surface.

The energy absorbed by the sample is obtained by multiplying the number of helium ions $N_{helim\ ions}$ by the energy of the particles coming into contact with the surface of the sample.

For instance, in this work a value R = 441.7 was determined for helium ions of 45 MeV initial energy. The charge measured in the ionisation chamber was q = 704.88 × 10^{-6} C for the irradiation of a zinc stearate pellet during 10 min. Then using the equation (Eq. (9)) and taking into account that each helium ions interacting with the pellet has a remaining energy of 7.9 MeV, the energy deposited in the sample is then E = 27,1 J.

It should be noticed that the path of the helium ion in zinc stearate is respectively 819 μm and 67 μm for energy of 34 MeV and 7.9 MeV. For an alpha particle emitted by plutonium (E_α = 5.2 MeV) this path is 34 μm. These path values have been calculated using SRIM-2008 software. In this way, all the incident particles are obviously implanted in zinc stearate pellets and each particle is going to lose its energy in a shell of a few micrometres depth. So even if the energy is not homogeneously deposited in the zinc stearate pellet, the energy transfer can be however described in term of a mean linear energy transfer (LET) along the track of the particle. The same remark is of course valid in the case of α particles emitted by plutonium dioxide. The values of mean LET are given in Table 5.

3. Results and discussion

3.1. Radiolytic yields of gaseous products

Analysis of the gases produced by irradiating zinc stearate has identified 5 main gases for each irradiation type: dihydrogen (H_2), carbon monoxide (CO), carbon dioxide (CO_2), methane (CH_4) and ethane (C_2H_6). Fig. 2 shows an example of the variation in the amount of each of the different gases released by the zinc stearate as a function of irradiation time in contact with PuO_2 for a plane-plane configuration.

Graphs equivalent to Fig. 2 have been drawn for each batch. Fig. 3 shows the example of the variation in the amount of H_2 produced during helium ion beam irradiation. The slope of the straight line tangent through the origin gives the gas formation yield.

The radiolytic yields of the main gases observed during radiolysis of zinc stearate are presented in Table 6 for the radiolysis tests with PuO_2, and in Table 7 for the external radiolysis tests.

It is possible that some of the H_2 produced comes from radiolysis of the water present on the surface of the PuO_2 (Gaillard, 2013; Jomard et al., 2014). The quantities of gas produced by radiolysis of the surface

Table 4
Comparison of dose rates absorbed by the zinc stearate in a mixture configuration with PuO_2 batches 4 and 5.

	$\dot{D}_{mean\ total}$ (J kg^{-1} s^{-1})
Batch 4	13.0
Batch 5	43.9

Table 5
LET of the particles used in this work for solid zinc stearate irradiation except (1) taken from Lebeau et al. (2017).

Particle	Path (μm)	LET (eV Å^{-1})
Gamma (1)	–	0.02
Helium beam (34 MeV)	819	4.15
Helium beam (7.9 MeV)	67	11.8
α from Pu decay (5.2 MeV)	34	15.3

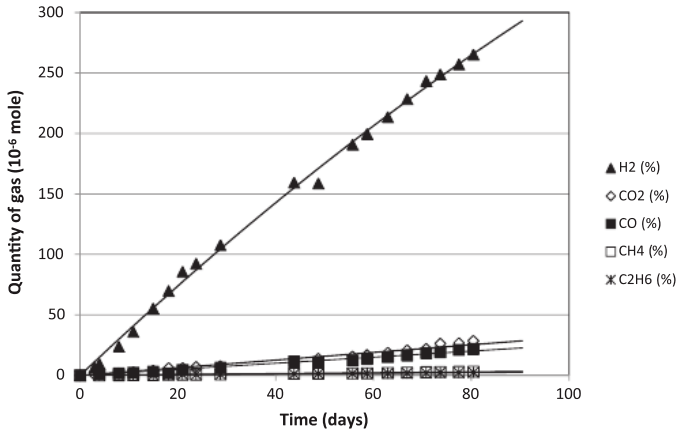

Fig. 2. Variation in the quantity of gases released through the radiolysis of zinc stearate by PuO_2 from batch 2 ($\dot{D}_\alpha$ = 6.75 J kg^{-1} s^{-1}, emitted by plutonium dioxide) in a plane-plane configuration under Ar/1% Ne atmosphere.

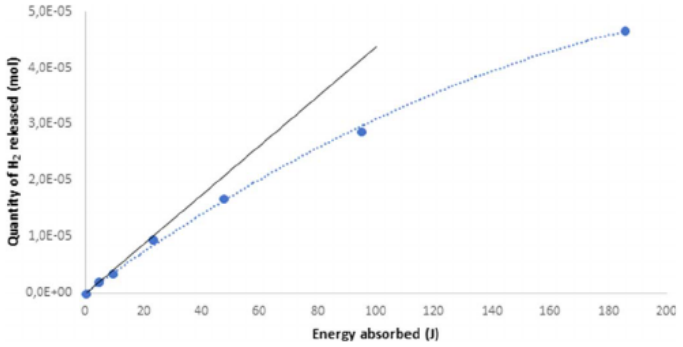

Fig. 3. Variation in the quantity of H_2 produced by radiolysis of zinc stearate as a function of absorbed energy during helium ion beam irradiations at 28 MeV under Ar/1% Ne atmosphere.

water represents between 4% and 16% of the total H_2 produced during the plane-plane irradiations, and between 1.1% and 1.5% for the powder mixtures. The H_2 generation yields given in Table 6 have been corrected to take account of this quantity produced by water radiolysis. The dihydrogen yield values obtained by the alpha irradiation of zinc stearate are consistent with the yields obtained for the degradation of polyethylene ($G_{H_2} \sim 3$–4×10^{-7} mol J^{-1}) (Hill and Whittaker, 2002; Khelidj et al., 2006).

These results show that zinc stearate has a behaviour close to polyethylene under irradiation. The aliphatic chain has a predominant effect on radiolytic behaviour of stearate over the carboxylate effect which influences energy transfers from aliphatic moiety to ester bonds. The presence of carboxylate function should decrease the quantity of radical reactions on the stearate chain, and decrease the quantity of H_2 produced compared to polyethylene. However, a significant decrease in H_2 radiolytic yields from zinc stearate compared to polyethylene is only observed for the mixture configuration. Moreover, a side experiment with stearic acid in a plane-plane configuration showed no effect on H_2 radiolytic yield ($G_0(H_2) = (3.5 \pm 0.6) \times 10^{-7}$ mol J^{-1}). On the opposite, CO_2 radiolytic yield was much higher with stearic acid ($G_0(CO_2) = (3.1 \pm 0.9) \times 10^{-7}$ mol J^{-1}) compared to zinc stearate ($G_0(CO_2) \sim (0.8 \pm 0.3) \times 10^{-7}$ mol J^{-1}). It clearly indicates that the presence of zinc stabilizes the carboxylic function. The fact that H_2 radiolytic yield for both zinc stearate and stearic acid is close to the one in polyethylene seems to indicate that the chain scission and radical reactions leading to the formation of H_2 are only slightly affected probably due to the length of the aliphatic chain. More details are given in Sections 3–5. The decrease in H_2 radiolytic yield for the mixture configurations could result from the degradation of zinc stearate to a higher extend and further side reactions of hydrogen and degradation products of zinc stearate on plutonium dioxide surface.

The formation of ethylene and acetylene was only observed during helium ion beam irradiation. The quantities are very low and the associated yields were not calculated.

3.2. *Effect of isotopy*

Different plutonium isotopies have been used to compare the radiolytic gas formation rates as a function of dose rate. Fig. 4 shows that the H_2 formation rate varies as a function of the PuO_2 batch and increases with the dose rate imposed by PuO_2. The gas emission kinetics depends on the PuO_2 isotope and the amount of energy absorbed by the zinc stearate.

The profile of the curves for batches 1 and 3, which is linear, differs from that for batches 2 and 5, which are the highest dose-emitting batches. The variation in these curves shows that the quantities of gas produced tends towards a limit over a very long time period, and thus for significant deposited doses. If the quantities of H_2 emitted are plotted as a function of the absorbed dose up to 10 MGy, linear curves are observed whatever the PuO_2 batch in contact with the zinc stearate (Fig. 5).

The results show that isotopy, and thus dose rate, has little effect on the gas generation yield (Table 6). Indeed, the gas generation kinetics

Table 6
Initial radiolytic yields of the main gases formed by radiolysis of zinc stearate in contact with PuO_2 (in 10^{-7} mol J^{-1}).

PuO_2 batch	Config.	Atmosphere	$G_0(H_2)$	$G_0(CO)$	$G_0(CO_2)$	$G_0(CH_4)$	$G_0(C_2H_6)$	α dose rate emitted by PuO_2 (J kg^{-1} s^{-1})	Absorbed Energy Rate (10^{-6} J s^{-1})
1	Plane-Plane	Ar/1% Ne	2.9 ± 0.5	0.40 ± 0.14	0.82 ± 0.24	0.055 ± 0.017	0.058 ± 0.021	2.02	86
2	Plane-Plane	Ar/1% Ne	4.1 ± 0.7	0.27 ± 0.10	0.35 ± 0.10	0.045 ± 0.014	0.035 ± 0.013	6.75	315
3	Plane-Plane	Ar/1% Ne	3.3 ± 0.5	0.23 ± 0.08	0.85 ± 0.25	0.043 ± 0.013	0.057 ± 0.020	2.40	86
4	Mixture	Ar/1% Ne	2.0 ± 0.5	0.17 ± 0.04	0.73 ± 0.14	0.027 ± 0.007	0.0008 ± 0.0003	4.88	260
5	Plane-Plane	Ar/1% Ne	4.1 ± 0.7	0.70 ± 0.25	0.89 ± 0.26	0.034 ± 0.010	0.0008 ± 0.0003	17.0	282
	Mixture	Ar/1% Ne	1.1 ± 0.3	0.27 ± 0.07	0.89 ± 0.17	0.025 ± 0.006	< detection limit		483

Table 7
Initial radiolytic yields of the main gases formed by $^4He^{2+}$ beam irradiation (in 10^{-7} mol J^{-1}).

Initial beam energy	Atmosphere	$G_0(H_2)$	$G_0(CO)$	$G_0(CO_2)$	$G_0(CH_4)$	$G_0(C_2H_6)$
28 MeV	Ar/1%Ne	4.2 ± 1.2	0.20 ± 0.06	1.5 ± 0.4	0.019 ± 0.005	0.010 ± 0.003
45 MeV	Ar/1%Ne	2.8 ± 0.4	0.063 ± 0.008	1.0 ± 0.1	0.014 ± 0.002	0.0098 ± 0.0013

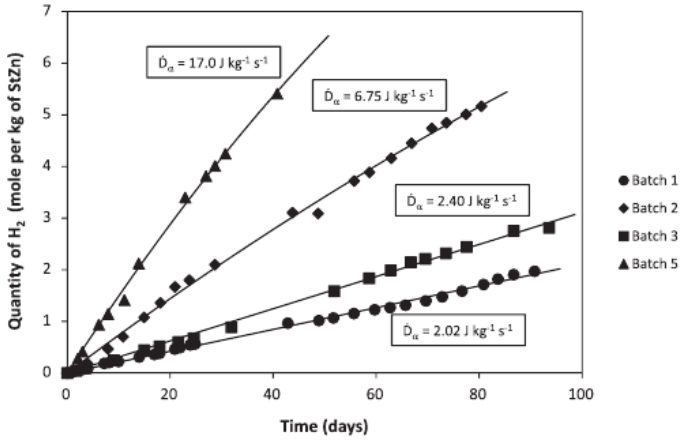

Fig. 4. Variation in the quantity of H_2 emitted by the zinc stearate in a plane-plane configuration as a function of the plutonium batch used (α dose rate emitted per mass unit of PuO_2).

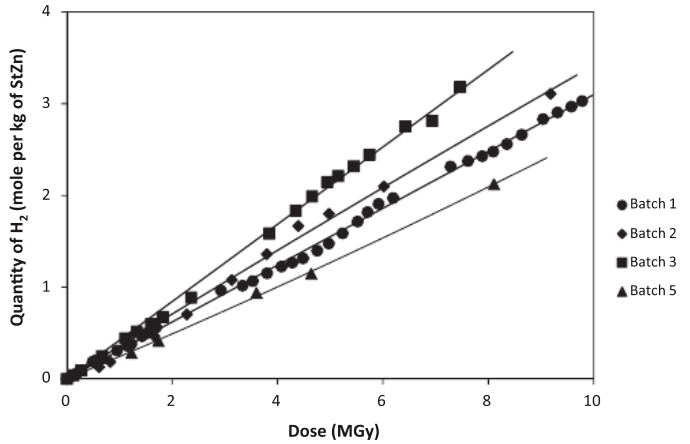

Fig. 5. Variation in the quantity of H_2 produced as a function of the absorbed dose in a plane-plane configuration for the 4 batches of PuO_2.

depend on the plutonium oxide dose rate used, but the different gas yields are in the same order of magnitude regardless of which PuO_2 batch is used. These results are consistent because the radiolytic degradation mechanism is the same. However, the CO_2 results for batch 2 and the C_2H_6 results for batch 5 are less than the others, for reasons which are as yet unexplained.

3.3. Effect of configuration

The comparison of the initial yields of gases (G_0) obtained as a function of the configuration used shows that the carbon dioxide yields are similar, whereas the yields of dihydrogen, carbon monoxide and alkanes are much lower (by a factor of 2–3 for H_2, CO and CH_4, and a factor of 50 for C_2H_6 in batch 4) in the mixture configuration (Table 6).

A strict comparison can be made on batch 5 which was used in both configurations. Differences in yield were observed on dihydrogen (factor 3.7) and carbon monoxide (factor 2.7). (Table 6).

These variations can be explained by the change in interaction between the PuO_2 and the zinc stearate as a function of the configuration. Essentially, the interface between the two materials differs depending on the configuration. The contact surface is much greater in the mixture configuration where each grain of zinc stearate is surrounded by several grains of PuO_2. The surface of the PuO_2 can be highly reactive with

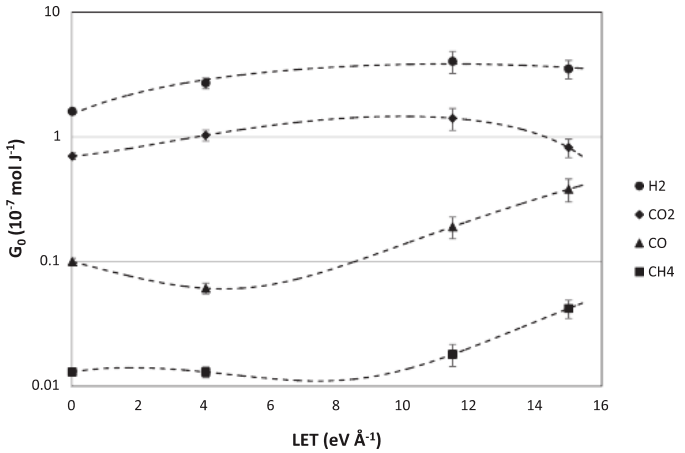

Fig. 6. Variation in gas formation yields as a function of the mean LET of the particles.

certain gases and can be modified by the reactions produced (Haschke et al., 2001).

The differences in yield can also be explained by the difference in density between the two configurations. In the plane-plane configuration, the gases generated can be contained in the pellets and therefore exhibited less mobility. This containment of gases tends to favour second order reactions.

3.4. Effect of LET

The external helium ion irradiations conducted in the CEMHTI cyclotron are representative, at similar energies, of irradiations performed with alpha particles emitted by plutonium decay. The gas generation yields obtained with the helium ions delivered at 28 MeV by the cyclotron (Table 7) are similar to those obtained during irradiations on zinc stearate pellets in a plane-plane configuration with the PuO_2 discs (Table 6). This is consistent since the energy end of the particles irradiating zinc stearate pellets are nearly the same in both case (7.9 MeV for external irradiation with helium ions and around 5.2 MeV for irradiation with α particles from plutonium) and the mean LET are pretty close (11.8 eV Å^{-1} and 15.2 eV Å^{-1} respectively). The yield results obtained with the helium ions at 45 MeV (*i.e* 34 MeV as initial remaining energy when interacting with zinc stearate) are lower, which could be explained by the lower mean LET (Table 5). The variation of the radiolytic yields is plotted as a function of the mean LET of the particle on Fig. 6. The radiolydic yield results obtained by Lebeau et al. (2017) under gamma irradiation were added to the results obtained in this study. These yields were determined after irradiations of 1 and 2 MGy. The ethane formation yield was not calculated. For the other four gases, the yield values obtained are less than those obtained during irradiations using helium ions or irradiations with PuO_2.

The general trend shows an increase in the mean LET resulting in a higher gas formation yield, which is consistent with the literature (Garaix, 2014; Roth and LaVerne, 2011). This increase may be due to the higher density of energy received by the irradiated material, resulting in an increase in the number and density of radicals produced. The high density of radicals causes an increase in the number of second order reactions.

3.5. Radiolytic degradation process

The radiolysis of zinc stearate by plutonium dioxide leads primarily to the formation of dihydrogen by cleaving C–H bonds along the chain. Since there is a very high number of C–H bonds in zinc stearate, because

of its long carbon chains, these bounds are then statistically likely to be cleaved. This bond cleavage causes the formation of $H^{\bullet}$ radicals which recombine to form H_2 and $C^{\bullet}$ radicals along the stearate carbon chain (Chang and Laverne, 2000). These radicals then recombine to form double bonds (disproportionation) or branches with adjacent chains (cross-linking).

Carbon products form in much lower quantities because they are derived from C–C bond cleavage which occurs randomly along the chain. There are fewer C–C bonds in proportion to C–H bonds, and there are even fewer C–CH_3 or C–CH_2–CH_3 bonds at the end of the chain due to the length of the stearate chain (C_{17}). Short-chain gaseous compounds are not necessarily formed during the first cleavage of the C–C bond, which can occur at any point along the chain. Chain cleavages are less favoured in this type of compound (alkane-polyethylene) (Dole and Patel, 1977). They are competing with the formation of double bonds, which appear to be quite numerous based on the H_2 yield. This may explain the much lower methane and ethane yield values compared to the other molecules.

The variations in H_2 and CH_4 yield are the same for a given configuration. These molecules can be formed in the same way from $H^{\bullet}$ and $CH_3^{\bullet}$ radicals (1′). In fact, these radicals can extract hydrogen atoms along the carbon chain (2′), recombine with $H^{\bullet}$ radicals (3′) or disproportionate to form double bonds (4′) (Chang and Laverne, 2000):

$$X\text{-}\,CH_2\text{-}CH_2\text{-}R \rightarrow X^{\bullet} + {}^{\bullet}CH\text{-}CH_2\text{-}R \quad (1')$$

$$X^{\bullet} + R\text{-}CH_2\text{-}CH_2\text{-}R' \rightarrow XH + R\text{-}{}^{\bullet}CH\text{-}CH_2\text{-}R' \quad (2')$$

$$X^{\bullet} + H^{\bullet} \rightarrow XH \quad (3')$$

$$X^{\bullet} + \text{-}CH_2\text{-}{}^{\bullet}CR\text{-} \rightarrow \text{-}CH{=}CR\text{-} + XH \quad (4')$$

Where X is H or CH_3.

The yield of these products (H_2 and CH_4) is 2 or 3 times greater in the dense (pellet) phase. Indeed, the probability of secondary reactions occurring is greater within a pellet.

The significant difference for ethane between the two configurations is difficult to explain. It is possible that the ethane was formed by successive cleavages along the aliphatic chain (5′) before recombining with an $H^{\bullet}$ radical (6′). Given that the density of the powder is lower, the probability of irradiating the same molecule several times is much lower.

$$R\text{-}CH_2\text{-}CH_2\text{-}R' \rightarrow R\text{-}{}^{\bullet}CH_2 + {}^{\bullet}CH_2\text{-}R' \quad (5')$$

$$R\text{-}{}^{\bullet}CH_2 + H^{\bullet} \rightarrow R\text{-}CH_3 \quad (6')$$

Carbon dioxide is the second major product formed during irradiation of zinc stearate. The oxygenated products can only be derived from the carboxylate function of the stearate since irradiation occurs in an inert atmosphere. The carboxylate function is more sensitive to interactions with ionizing radiation due to its high electronic density. Far less CO_2 is released for zinc stearate than is generally reported for carboxylic acids (Nawar, 1978). In carboxylic acids, the first radical formed (predominantly) is the radical $RCOO^{\bullet}$ generated by the cleavage of the O–H bond which occurs easily after excitation of the molecule (7′), due to the lability of the acid proton and the hydrogen bonds between the acids (8′). Moreover, it is probable that the tetrahedral structure around the zinc ion stabilises the carboxylate function and makes it less accessible.

$$RCOOH \xrightarrow{\alpha} RCOOH^{*+} \quad (7')$$

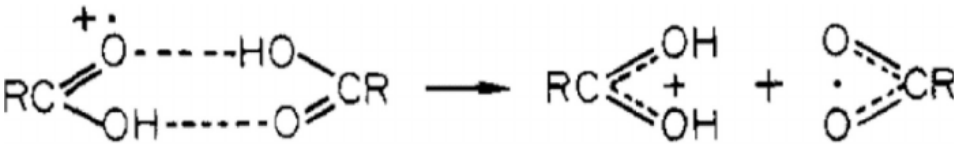

(8′)

The CO_2 yield is the same in both configurations, since it is formed by a first order reaction mechanism (Nawar, 1978). As shown during the radiolysis of carboxylic acids, CO_2 is formed by a radical decarboxylation reaction $RC(=O)O^{\bullet}$ (9′). This rearrangement is very rapid (Nawar, 1978):

$$RC(=O)O^{\bullet} \rightarrow R^{\bullet} + CO_2 \quad (9')$$

It is generally reported that less carbon monoxide is formed than carbon dioxide in the radiolysis of carboxylic acid (Nawar, 1978; Spinks, 1990). However, the CO formation mechanism is more complex to determine, hence the difficulty in substantiating the difference in yields observed as a function of the configuration. No mechanism has been found satisfying to explain such a variation in carbon monoxide yield.

4. Conclusion

The gas generation yields obtained by helium ion beam irradiation show that the zinc stearate radiolysis process seems to be similar to that determined by alpha radiolysis. This process is used to simulate Pu irradiations without contaminating the target material (no contact with the PuO_2 powder) which allows us to characterise the irradiated material and enhance our knowledge of the radiolysis mechanism.

The results obtained by varying the plutonium isotope in contact with the zinc stearate shows that isotopy has little effect on the gas formation yields. It would therefore be reasonable to consider that the degradation of zinc stearate will be the same regardless of which batch of PuO_2 is used; only the rate of degradation will increase with the dose rate. This constancy of G_0 allows us to extrapolate the results to the use of plutonium containing a higher quantity of ^{238}Pu and with a much stronger dose rate than that used in this study. This initial study on gases emitted during radiolysis must nevertheless be completed by further analysis of the irradiated solid compound to identify the different molecules formed and to propose a more complete radiolytic degradation mechanism for zinc stearate.

Acknowledgments

This work was supported by the MINOS Program (Materials Innovation for Nuclear Optimized Systems) of the CEA Nuclear Energy Division both in the department of radiochemistry and processes and the department of fuel study.

The authors like to express their gratitude for the CEMHTI facility teams for their technical support in this study.

The authors are especially grateful to Mr. Stephane ESNOUF (CEA/DANS/DPC – Saclay site) for his help and constructive discussions in

calculating the dose rate in zinc stearate irradiation with plutonium dioxide.

References

Balanzat, E., Betz, N., Bouffard, S., 1995. Swift heavy ion modification of polymers. Nucl. Instrum. Methods Phys. Res. Sect. B Beam Interact. Mater. At. 105, 46–54. http://dx.doi.org/10.1016/0168-583X(95)00521-8.

Chang, Z., Laverne, J.A., 2000. Hydrogen production in γ-ray and helium-ion radiolysis of polyethylene, polypropylene, poly(methyl-methacrylate), and polystyrene. J. Polym. Sci. Part Polym. Chem. 38, 1656–1661. http://dx.doi.org/10.1002/(SICI)1099-0518(20000501)38:9<1656::AID-POLA31>3.0.CO;2-S.

Dole, M., Patel, V.M., 1977. Comparison of irradiation crosslinking and chain scission in extended chain and bulk film samples of linear polyethylene. Radiat. Phys. Chem. 9, 433–444. http://dx.doi.org/10.1016/0146-5724(77)90159-5.

Ferry, M., Ngono-Ravache, Y., Aymes-Chodur, C., Clochard, M.C., Coqueret, X., Cortella, L., Pellizzi, E., Rouif, S., Esnouf, S., 2016. Ionizing radiation effects in polymers. In: Reference Module in Materials Science and Materials Engineering. Elsevier. ⟨http://dx.doi.org/10.1016/B978-0-12-803581-8.02095-6⟩.

Gaillard, J., 2013. Réactivité de l'eau à la surface des oxydes mixtes (U,Pu)O_2 (Thèse de l'Université Montpellier 2). (in French).

Garaix, G., 2014. Radiolyse alpha de solutions aqueuses d'acide nitrique (Thèse de l'Université Montpellier 2). (in French).

Haschke, J.M., Allen, T.H., Morales, L.A., 2001. Reactions of plutonium dioxide with water and hydrogen–oxygen mixtures: mechanisms for corrosion of uranium and plutonium. J. Alloy. Compd. 314, 78–91. http://dx.doi.org/10.1016/S0925-8388(00)01222-6.

Hill, D.J.T., Whittaker, A.K., 2002. Radiation chemistry of polymers. In: Encyclopedia of Polymer Science and Technology. John Wiley & Sons, Inc.,

Jomard, G., Bottin, F., Geneste, G., 2014. Water adsorption and dissociation on the PuO_2(110) surface. J. Nucl. Mater. 451, 28–34. http://dx.doi.org/10.1016/j.jnucmat.2014.03.012.

Khelidj, N., Colin, X., Audouin, L., Verdu, J., Monchy-Leroy, C., Prunier, V., 2006. Oxidation of polyethylene under irradiation at low temperature and low dose rate. Part I. The case of "pure" radiochemical initiation. Polym. Degrad. Stab. 91, 1593–1597. http://dx.doi.org/10.1016/j.polymdegradstab.2005.09.011.

Lebeau, D., Beuvier, L., Cornaton, M., Miserque, F., Tabarant, M., Esnouf, S., Ferry, M., 2015. Aging of magnesium stearate under high doses gamma irradiation and oxidative conditions. J. Nucl. Mater. 460, 130–138. http://dx.doi.org/10.1016/j.jnucmat.2015.02.016.

Lebeau, D., Esnouf, S., Gracia, J., Audubert, F., Ferry, M., 2017. New generation of nuclear fuels: stability of different stearates under high doses gamma irradiation in the manufacturing process. J. Nucl. Mater. 490, 288–298. http://dx.doi.org/10.1016/j.jnucmat.2017.04.029.

Nawar, W.W., 1978. Reaction mechanisms in the radiolysis of fats: a review. J. Agric. Food Chem. 26, 21–25. http://dx.doi.org/10.1021/jf60215a079.

Pizette, P., Martin, C.L., Delette, G., Sornay, P., Sans, F., 2010. Compaction of aggregated ceramic powders: from contact laws to fracture and yield surfaces. Powder Technol. 198, 240–250. http://dx.doi.org/10.1016/j.powtec.2009.11.013.

Roth, O., LaVerne, J.A., 2011. Effect of pH on H_2O_2 production in the radiolysis of water. J. Phys. Chem. A 115, 700–708. http://dx.doi.org/10.1021/jp1099927.

Spinks, J.W.T., Woods, R.J., 1990. An Introduction to Radiation Chemistry, Third ed. John Wiley Sons Inc.

Vladimirova, M.V., Kulikov, I.A., 2012. Formation of H_2 and O_2 in radiolysis of water sorbed on PuO_2. Radiochemistry 44, 86–90. http://dx.doi.org/10.1023/A:1014839621040.